



Effect of internal optical loss on the modulation bandwidth of a quantum dot laser

Yuchang Wu, Robert A. Suris, and Levon V. Asryan

Citation: [Applied Physics Letters](#) **100**, 131106 (2012); doi: 10.1063/1.3697683

View online: <http://dx.doi.org/10.1063/1.3697683>

View Table of Contents: <http://scitation.aip.org/content/aip/journal/apl/100/13?ver=pdfcov>

Published by the [AIP Publishing](#)

Articles you may be interested in

[Effect of excited states on the ground-state modulation bandwidth in quantum dot lasers](#)

Appl. Phys. Lett. **102**, 191102 (2013); 10.1063/1.4804994

[Intersubband absorption of quantum cascade laser structures and its application to laser modulation](#)

Appl. Phys. Lett. **92**, 211108 (2008); 10.1063/1.2937207

[Theoretical study on high-speed modulation of Fabry-Pérot and distributed-feedback quantum-dot lasers: K-factor-limited bandwidth and 10 Gbit/s eye diagrams](#)

J. Appl. Phys. **101**, 013108 (2007); 10.1063/1.2407259

[Limitations on standard procedure of determining internal loss and efficiency in quantum dot lasers](#)

J. Appl. Phys. **99**, 013102 (2006); 10.1063/1.2159072

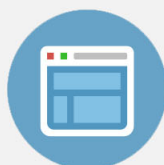
[Optical loss and lasing characteristics of high-quality-factor AlGaAs microdisk resonators with embedded quantum dots](#)

Appl. Phys. Lett. **86**, 151106 (2005); 10.1063/1.1901810

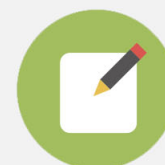


Re-register for Table of Content Alerts

Create a profile.



Sign up today!



Effect of internal optical loss on the modulation bandwidth of a quantum dot laser

Yuchang Wu,^{1,a)} Robert A. Suris,^{2,b)} and Levon V. Asryan^{1,c)}

¹Virginia Polytechnic Institute and State University, Blacksburg, Virginia 24061, USA

²Ioffe Physico-Technical Institute, St. Petersburg 194021, Russia

(Received 10 February 2012; accepted 6 March 2012; published online 26 March 2012)

We show that the internal optical loss, which increases with free-carrier density in the waveguide region, considerably reduces the modulation bandwidth $\omega_{-3\text{dB}}$ of a quantum dot laser. At a certain optimum value J_0^{opt} of the dc component of the injection current density, the maximum bandwidth $\omega_{-3\text{dB}}^{\text{max}}$ is attained and the modulation response function becomes as flat as possible. With internal loss cross-section σ_{int} increasing and approaching its maximum tolerable value, $\omega_{-3\text{dB}}^{\text{max}}$ decreases and becomes zero. As with J_0^{opt} , there also exists the optimum cavity length, at which $\omega_{-3\text{dB}}$ is highest; the larger is σ_{int} , the longer is the optimum cavity. © 2012 American Institute of Physics. [<http://dx.doi.org/10.1063/1.3697683>]

The optical output in edge-emitting semiconductor lasers is provided by photons leaving the cavity through its mirrors. In addition to this useful output loss, there is also parasitic loss of photons, which occurs within the laser cavity and, for this reason, is termed internal optical loss. There can be several mechanisms for internal loss,^{1–6} such as free-carrier absorption, intervalence band absorption, and scattering at rough surfaces. While there have been studies of the effect of internal loss on the threshold and power characteristics of semiconductor lasers with a quantum-confined active region and, particularly, quantum dot (QD) lasers,^{7–9} no consideration of the dynamic properties of QD lasers in the presence of internal loss has been given so far. In this work, we study the modulation response of a QD laser taking into account the carrier-density-dependent internal loss in the optical confinement layer (OCL). To mainly focus on the effect of internal loss, we do not consider here some other factors, among them the carrier capture delay from the OCL into QDs,¹⁰ which also affect the modulation bandwidth of a laser.

To consider a direct modulation of the laser output by alternating current (ac), we use the small-signal analysis^{11–17} and hence we assume that the ac component δj of the injection current density is small. For small variations $\delta \dots$ of the corresponding quantities (around their steady-state values) caused by δj , we have the following rate equations:

$$\frac{\partial}{\partial t}(\delta n) = \frac{\delta j}{eb} - \delta R_{\text{non-stim}} - \delta R_{\text{stim}}, \quad (1)$$

$$\frac{\partial}{\partial t}(\delta n_{\text{ph}}) = \delta R_{\text{stim}} - \delta R_{\text{loss}}, \quad (2)$$

where $n = n_{\text{act}} + n_{\text{OCL}}$, n_{act} and n_{OCL} are the carrier densities in the active region and OCL, respectively, n_{ph} is the photon density (per unit volume of the OCL) in the lasing mode, e is the electron charge, b is the thickness of the OCL, and

$R_{\text{non-stim}}$ is the rate of the processes of non-stimulated recombination of carriers in the active region and OCL.

In Eqs. (1) and (2), the rate of stimulated recombination of carriers, which is the same as the rate of stimulated emission of photons, is

$$R_{\text{stim}} = v_g g n_{\text{ph}}, \quad (3)$$

where v_g is the group velocity of light and g is the modal gain of the laser.

The photon loss rate in Eq. (2) is the sum of the useful output (mirror) and parasitic (internal) loss rates,

$$R_{\text{loss}} = v_g (\beta + \alpha_{\text{int}}) n_{\text{ph}}, \quad (4)$$

where $\beta = (1/L) \ln(1/R)$ is the mirror loss coefficient, L is the cavity length, and R is the mirror reflectivity.

In the general case, the internal loss coefficient can be presented as^{7–9}

$$\alpha_{\text{int}} = \alpha_0 + \sigma_{\text{int}} n_{\text{OCL}}, \quad (5)$$

where the constant component α_0 accounts for scattering at rough surfaces and free-carrier absorption in the cladding layers, and the component $\sigma_{\text{int}} n_{\text{OCL}}$ describes free-carrier and intervalence band absorption in the OCL with σ_{int} being the effective cross-section for these absorption loss processes.

As seen from Eq. (5), α_{int} will vary with time through such variation in the free-carrier density n_{OCL} caused by the ac current. Hence, as seen from Eqs. (4) and (5), the temporal variation of the photon loss rate will be due to such variation of not only the photon density n_{ph} but n_{OCL} as well.

Considering a time-harmonic ac injection current density, $\delta j = \delta j_m \exp(i\omega t)$, we find from Eqs. (1) and (2) the frequency-dependent amplitude $\delta n_{\text{ph-m}}(\omega)$ of the time-harmonic photonic density and then the modulation response function $H(\omega)$,

$$H(\omega) = \frac{|\delta n_{\text{ph-m}}(\omega)|^2}{|\delta n_{\text{ph-m}}(0)|^2} = \frac{\omega_0^4}{(\omega^2 - \omega_0^2)^2 + 4\Gamma_{\text{dec}}^2 \omega^2}. \quad (6)$$

^{a)}Electronic mail: yuchangw@vt.edu.

^{b)}Electronic mail: suris@theory.ioffe.ru.

^{c)}Electronic mail: asryan@vt.edu.

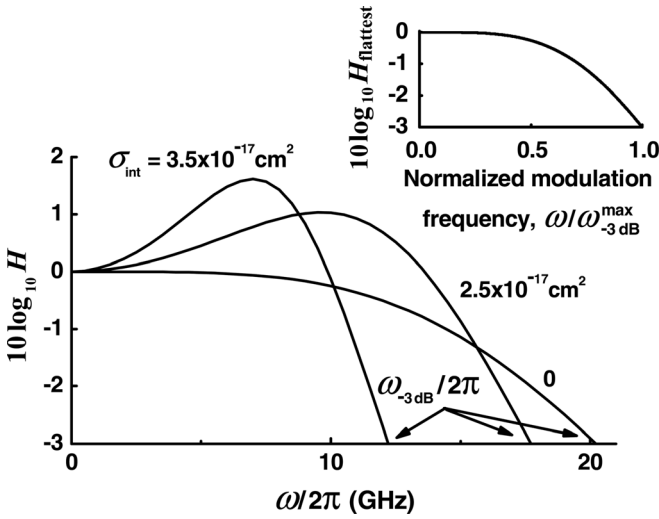


FIG. 1. Modulation response function at different values of the internal loss cross-section σ_{int} . For our calculations, room-temperature operation of a GaInAsP structure of Ref. 20 with a single layer of QDs lasing near 1.55 μm is considered; 10% QD-size fluctuations are assumed; $g^{\text{max}} = 29.52 \text{ cm}^{-1}$, $\alpha_0 = 0$ and $L = 1.139 \text{ mm}$. For all the three curves, the dc component of the injection current density $j_0 = 64 \text{ kA/cm}^2$; for the case of no internal loss, this value of j_0 is equal to j_0^{opt} and that is why the response function is flattest. The inset shows the flattest response function given by Eq. (15) vs. normalized modulation frequency $\omega/\omega_{-3\text{dB}}^{\text{max}}$; using this universal dependence and Eq. (12) for $\omega_{-3\text{dB}}^{\text{max}}$, the flattest response function at a non-zero σ_{int} can be easily plotted.

While the shape of $H(\omega)$ depends strongly on the internal loss (Fig. 1), as a function of the frequency ω of direct modulation and parameters Γ_{dec} and ω_0 , expression (6) is the same as for the case of no internal loss.¹⁸

The decay rate of relaxation oscillations is given by

$$\Gamma_{\text{dec}} = \frac{1}{2} \left(\frac{1}{\tau_{\text{non-stim}}^{\text{dif}}} + v_g G^{\text{dif}} n_{\text{ph},0} \right), \quad (7)$$

where $\tau_{\text{non-stim}}^{\text{dif}} = (\partial R_{\text{non-stim},0}/\partial n_0)^{-1}$ is the effective differential non-stimulated recombination time, $G^{\text{dif}} = \partial g_0/\partial n_0$ is the effective differential gain, $g_0 = g^{\text{max}} (2f_{n,0} - 1)$ is the modal gain, g^{max} is the maximum value of the modal gain, and $f_{n,0}$ is the confined-carrier level occupancy in a QD. Except for α_0 and ω_0 , “0” in the subscripts of all the other quantities denotes their steady-state values.

In terms of the quantities $\tau_{\text{non-stim}}^{\text{dif}}$, G^{dif} , and $n_{\text{ph},0}$, expression (7) is also the same as for the case of no internal loss.¹⁸ Each of these quantities is, however, affected by the internal loss.

For ω_0 entering into Eq. (6), we have

$$\omega_0 = \sqrt{v_g G^{\text{dif}} n_{\text{ph},0} \frac{1}{\tau_{\text{ph},0}} \sqrt{1 - \frac{\partial \alpha_{\text{int},0}}{\partial g_0}}}, \quad (8)$$

where $\tau_{\text{ph},0}$ is the photon lifetime in the cavity,

$$\tau_{\text{ph},0} = \frac{1}{v_g(\beta + \alpha_{\text{int},0})} = \frac{1}{v_g(\beta + \alpha_0 + \sigma_{\text{int}} n_{\text{OCL},0})}. \quad (9)$$

Due to the internal loss, $\tau_{\text{ph},0}$ depends on the free-carrier density $n_{\text{OCL},0}$ in the OCL.

For the modulation bandwidth, which is defined as the -3 dB bandwidth [$10 \log_{10} H(\omega_{-3 \text{ dB}}) = -3$, see Fig. 1], we derived

$$\begin{aligned} \omega_{-3 \text{ dB}} &= \sqrt{\sqrt{\omega_{\text{peak}}^4 + (r-1)\omega_0^4 + \omega_{\text{peak}}^2}} \\ &= \sqrt{\sqrt{(\omega_0^2 - 2\Gamma_{\text{dec}}^2)^2 + (r-1)\omega_0^4 + (\omega_0^2 - 2\Gamma_{\text{dec}}^2)},} \end{aligned} \quad (10)$$

where $r = 10^{0.3} \approx 1.995$ and

$$\omega_{\text{peak}} = \sqrt{\omega_0^2 - 2\Gamma_{\text{dec}}^2}. \quad (11)$$

The steady-state photon density $n_{\text{ph},0}$, entering into Eqs. (7) and (8), is a function of the dc component j_0 of the injection current density (the relationship between $n_{\text{ph},0}$ and j_0 is given by the light-current characteristic). Consequently, all the quantities Γ_{dec} , ω_0 , ω_{peak} , $\omega_{-3 \text{ dB}}$, and the response function $H(\omega)$ depend on j_0 as well.

When $H(\omega)$ has a peak (which occurs only for a certain range of values of the dc component j_0 of the injection current density), Eq. (11) presents the frequency of the peak. Equation (10) for $\omega_{-3 \text{ dB}}$ holds also for those j_0 at which there is no peak in $H(\omega)$ – in that case too, ω_{peak} is formally given by Eq. (11) but the difference $\omega_0^2 - 2\Gamma_{\text{dec}}^2$ in Eq. (11) is negative.

With increasing j_0 above the threshold current density j_{th} , the modulation bandwidth increases from zero, approaches its maximum value $\omega_{-3 \text{ dB}}^{\text{max}}$ (marked by the symbol “x” in Fig. 2) at a certain optimum dc current density j_0^{opt} , then decreases and will asymptotically approach its saturation value. At $j_0 = j_0^{\text{opt}}$, when the maximum bandwidth $\omega_{-3 \text{ dB}}^{\text{max}}$ is attained, the peak of the response function occurs at $\omega_{\text{peak}} = 0$ and the response function becomes as flat as possible (Fig. 1).

Analyzing Eq. (10) for $\omega_{-3 \text{ dB}}$ as a function of j_0 , we obtained the following expression for $\omega_{-3 \text{ dB}}^{\text{max}}$:

$$\omega_{-3 \text{ dB}}^{\text{max}} \approx \frac{\sqrt{2}}{\tau_{\text{ph},0}} \left(1 - \frac{\partial \alpha_{\text{int},0}}{\partial g_0} \right) = \frac{\sqrt{2}}{\tau_{\text{ph},0}} \left[1 - \frac{\sigma_{\text{int}} n_1}{2g^{\text{max}}(1-f_{n,0})^2} \right], \quad (12)$$

where we used Eq. (5) for α_{int} and the equation $n_{\text{OCL}} = n_1 f_n / (1 - f_n)$ (Eq. (3) of Ref. 19) relating the free-carrier

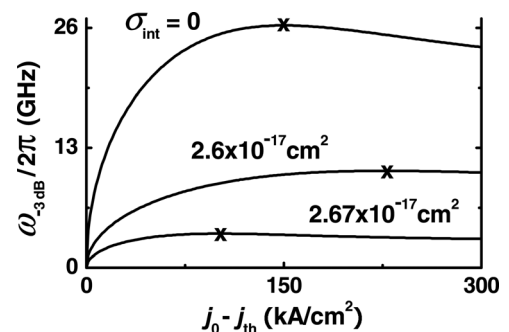


FIG. 2. Modulation bandwidth $\omega_{-3\text{dB}}/2\pi$ vs. excess of the dc component of the injection current density over the threshold current density at different values of σ_{int} . $\alpha_0 = 3 \text{ cm}^{-1}$ and $L = 1.139 \text{ mm}$. The “x” symbol marks the maximum point (j_0^{opt} , $\omega_{-3\text{dB}}^{\text{max}}$) on each curve.

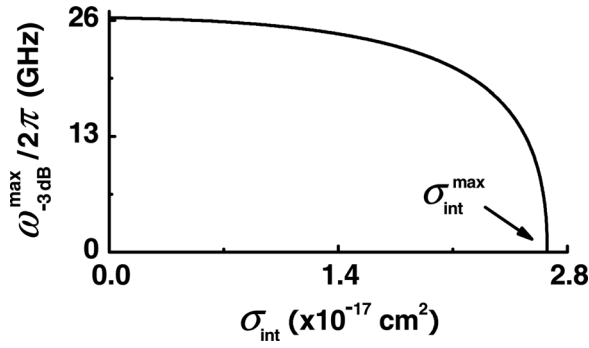


FIG. 3. Maximum modulation bandwidth $\omega_{-3\text{dB}}^{\text{max}}/2\pi$ vs. internal loss cross-section σ_{int} . $\alpha_0 = 3 \text{ cm}^{-1}$ and $L = 1.139 \text{ mm}$; $\sigma_{\text{int}}^{\text{max}} = 2.677 \times 10^{-17} \text{ cm}^2$.

density in the OCL n_{OCL} to the confined-carrier level occupancy in a QD f_n . The quantity $n_1 = N_c^{\text{OCL}} \exp(-E_n/T)$ characterizes the intensity of thermally excited escape of carriers from a QD to the OCL, N_c^{OCL} is the effective density of states in the OCL, E_n is the carrier excitation energy from a QD, and T is the temperature (in units of energy).

Due to the free-carrier-density-dependent internal loss, the confined-carrier level occupancy in a QD $f_{n,0}$ entering into Eq. (12) is itself a function of σ_{int} . In Ref. 7, the following expression was derived for $f_{n,0}$ from the steady-state lasing condition (equality of the gain to the total loss):

$$f_{n,0} = \frac{1}{4} \left(3 + \frac{\beta + \alpha_0 - \sigma_{\text{int}} n_1}{g^{\text{max}}} \right) - \sqrt{\frac{1}{16} \left(3 + \frac{\beta + \alpha_0 - \sigma_{\text{int}} n_1}{g^{\text{max}}} \right)^2 - \frac{1}{2} \left(1 + \frac{\beta + \alpha_0}{g^{\text{max}}} \right)}. \quad (13)$$

Fig. 3 shows $\omega_{-3\text{dB}}^{\text{max}}/2\pi$ vs. σ_{int} . As seen from Eq. (12), Fig. 3 and also Fig. 2, $\omega_{-3\text{dB}}^{\text{max}}$ is highest for the case of no free-carrier-density-dependent internal loss ($\sigma_{\text{int}} = 0$). With σ_{int} increasing and approaching a certain maximum tolerable value $\sigma_{\text{int}}^{\text{max}}$, $\omega_{-3\text{dB}}^{\text{max}}$ decreases and becomes zero. Using Eq. (13) for $f_{n,0}$ in Eq. (12) for $\omega_{-3\text{dB}}^{\text{max}}$ and equalizing the latter to zero, we obtain the following expression for the critical tolerable cross-section of internal loss (see also Ref. 19):

$$\sigma_{\text{int}}^{\text{max}} = \frac{(\sqrt{2g^{\text{max}}} - \sqrt{\beta + \alpha_0 + g^{\text{max}}})^2}{n_1}. \quad (14)$$

For $\sigma_{\text{int}} > \sigma_{\text{int}}^{\text{max}}$, the lasing is not attainable in the structure and, naturally, no direct modulation is possible.

While $\omega_{-3\text{dB}}^{\text{max}}$ depends strongly on σ_{int} , the flattest response function (the response function at $j_0 = j_0^{\text{opt}}$) is universal in terms of the normalized modulation frequency $\omega/\omega_{-3\text{dB}}^{\text{max}}$ (the inset in Fig. 1),

$$H_{\text{flattest}}(\omega/\omega_{-3\text{dB}}^{\text{max}}) = \frac{1}{1 + (\omega/\omega_{-3\text{dB}}^{\text{max}})^4}. \quad (15)$$

As seen from Fig. 4, as a function of the cavity length, $\omega_{-3\text{dB}}^{\text{max}}$ has a maximum. With increasing L from the shortest tolerable cavity length required for lasing,¹⁹ $\omega_{-3\text{dB}}^{\text{max}}$ increases from zero, approaches its highest value $\omega_{-3\text{dB}}^{\text{highest}}$ at a certain optimum cavity length L^{opt} , and then decreases. L^{opt} depends on σ_{int} – the larger is σ_{int} , the longer should be the optimum cavity. When

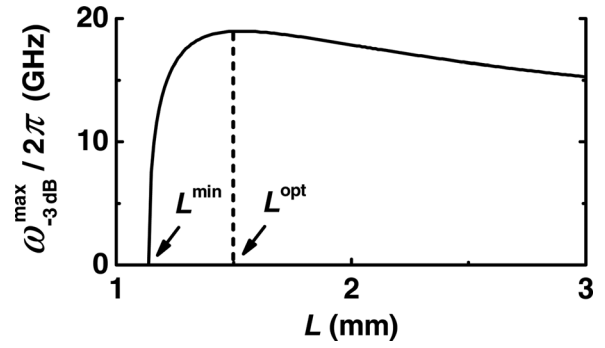


FIG. 4. Maximum modulation bandwidth $\omega_{-3\text{dB}}^{\text{max}}/2\pi$ vs. cavity length L . $\alpha_0 = 3 \text{ cm}^{-1}$ and $\sigma_{\text{int}} = 2.67 \times 10^{-17} \text{ cm}^2$; $L^{\text{opt}} = 1.5 \text{ mm}$.

σ_{int} is small [so small that the second terms in the brackets in the right-hand sides of Eqs. (16) and (17) are much less compared to unity], the analysis of Eq. (12) for $\omega_{-3\text{dB}}^{\text{max}}$ as a function of L yields the following expressions for L^{opt} and $\omega_{-3\text{dB}}^{\text{highest}}$:

$$L^{\text{opt}} \approx L_0^{\text{min}} \left(1 + \frac{g^{\text{max}}}{g^{\text{max}} - \alpha_0} \sqrt[3]{\frac{4\sigma_{\text{int}} n_1}{g^{\text{max}}}} \right) = \frac{\ln(1/R)}{g^{\text{max}} - \alpha_0} \left(1 + \frac{g^{\text{max}}}{g^{\text{max}} - \alpha_0} \sqrt[3]{\frac{4\sigma_{\text{int}} n_1}{g^{\text{max}}}} \right), \quad (16)$$

$$\omega_{-3\text{dB}}^{\text{highest}} \approx \omega_{-3\text{dB}}^{\text{highest}} \Big|_{\sigma_{\text{int}}=0} \left(1 - \frac{3}{2} \sqrt[3]{\frac{4\sigma_{\text{int}} n_1}{g^{\text{max}}}} \right) = \sqrt{2} v_g g^{\text{max}} \left(1 - \frac{3}{2} \sqrt[3]{\frac{4\sigma_{\text{int}} n_1}{g^{\text{max}}}} \right), \quad (17)$$

where L_0^{min} and $\omega_{-3\text{dB}}^{\text{highest}} \Big|_{\sigma_{\text{int}}=0}$ are the shortest tolerable cavity length and the highest bandwidth, respectively, when $\sigma_{\text{int}} = 0$.

The highest modulation bandwidth $\omega_{-3\text{dB}}^{\text{highest}}/2\pi$ is shown against σ_{int} in Fig. 5. As seen from the figure, in the ideal case of no free-carrier-density-dependent internal loss in the OCL (and also no carrier capture delay from the OCL into QDs), $(\omega_{-3\text{dB}}^{\text{highest}} \Big|_{\sigma_{\text{int}}=0})/2\pi$ is about 60 GHz in a GaInAsP structure of Ref. 20 used for our calculations here. In the presence of such a loss, $\omega_{-3\text{dB}}^{\text{highest}}/2\pi$ is, however, considerably reduced and becomes vanishing as σ_{int} approaches its maximum tolerable value (Fig. 5).

In conclusion, the free-carrier-density-dependent internal optical loss in the waveguide region has been shown to

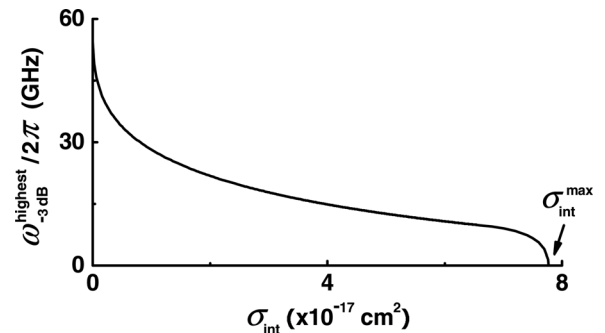


FIG. 5. Highest modulation bandwidth $\omega_{-3\text{dB}}^{\text{highest}}/2\pi$ vs. internal loss cross-section σ_{int} . $\alpha_0 = 3 \text{ cm}^{-1}$. $\sigma_{\text{int}}^{\text{max}}$ in the figure corresponds to $L = \infty$ and that is why it is larger than in Fig. 3.

considerably reduce the modulation bandwidth $\omega_{-3\text{ dB}}$ of a QD laser. At a certain optimum value J_0^{opt} of the dc component of the injection current density, the maximum bandwidth $\omega_{-3\text{ dB}}^{\text{max}}$ is attained and the response function becomes as flat as possible. While $\omega_{-3\text{ dB}}^{\text{max}}$ depends strongly on the effective cross-section σ_{int} of internal absorption loss processes (decreases and becomes zero at the maximum tolerable value of σ_{int}), the flattest response function is universal in terms of the normalized modulation frequency $\omega/\omega_{-3\text{ dB}}^{\text{max}}$. As with J_0^{opt} , there also exists the optimum cavity length, at which $\omega_{-3\text{ dB}}$ is highest; the larger is σ_{int} , the longer should be the optimum cavity.

L.V.A. and Y.W. acknowledge the U.S. Army Research Office (Grant No. W911-NF-08-1-0462), Y.W. also acknowledges the China Scholarship Council, and R.A.S. acknowledges the Russian Foundation for Basic Research (Grant No. 11-02-00573) and the Program “Fundamental Research in Nanotechnology and Nanomaterials” of the Presidium of the Russian Academy of Sciences for support of this work.

¹G. P. Agrawal and N. K. Dutta, *Long-Wavelength Semiconductor Lasers* (Van Nostrand, New York, 1986), p. 474.

- ²D. Z. Garbuzov, A. V. Ovchinnikov, N. A. Pikhin, Z. N. Sokolova, I. S. Tarasov, and V. B. Khalfin, *Sov. Phys. Semicond.* **25**, 560 (1991).
- ³C. H. Henry, R. A. Logan, F. R. Merritt, and J. P. Luongo, *IEEE J. Quantum Electron.* **19**, 947 (1983).
- ⁴M. Asada, A. Kameyama, and Y. Suematsu, *IEEE J. Quantum Electron.* **20**, 745 (1984).
- ⁵J. J. Lee, L. J. Mawst, and D. Botez, *J. Cryst. Growth* **249**, 100 (2003).
- ⁶D. A. Ackerman, G. E. Shtengel, M. S. Hybertsen, P. A. Morton, R. F. Kazarinov, T. Tanbun-Ek, and R. A. Logan, *IEEE J. Sel. Top. Quantum Electron.* **1**, 250 (1995).
- ⁷L. V. Asryan and S. Luryi, *Appl. Phys. Lett.* **83**, 5368 (2003).
- ⁸L. V. Asryan, *Appl. Phys. Lett.* **88**, 073107 (2006).
- ⁹L. Jiang and L. V. Asryan, *Laser Phys. Lett.* **4**, 265 (2007).
- ¹⁰L. V. Asryan, Y. Wu, and R. A. Suris, *Appl. Phys. Lett.* **98**, 131108 (2011).
- ¹¹T. Ikegami and Y. Suematsu, *Proc. IEEE* **55**, 122 (1967).
- ¹²T. L. Paoli and J. E. Ripper, *Proc. IEEE* **58**, 1457 (1970).
- ¹³M. J. Adams, *Opto-electronics* **5**, 201 (1973).
- ¹⁴R. F. Kazarinov and R. A. Suris, *Sov. Phys. JETP* **39**, 522 (1974).
- ¹⁵C. B. Su and V. A. Lanzisera, *IEEE J. Quantum Electron.* **22**, 1568 (1986).
- ¹⁶R. Olshansky, P. Hill, V. Lanzisera, and W. Powazinik, *IEEE J. Quantum Electron.* **23**, 1410 (1987).
- ¹⁷R. Nagarajan, M. Ishikawa, T. Fukushima, R. S. Geels, and J. E. Bowers, *IEEE J. Quantum Electron.* **28**, 1990 (1992).
- ¹⁸L. V. Asryan and R. A. Suris, *Appl. Phys. Lett.* **96**, 221112 (2010).
- ¹⁹L. V. Asryan and S. Luryi, *IEEE J. Quantum Electron.* **40**, 833 (2004).
- ²⁰L. V. Asryan and R. A. Suris, *Semicond. Sci. Technol.* **11**, 554 (1996).